

See discussions, stats, and author profiles for this publication at: <https://www.researchgate.net/publication/244285610>

Molecular geometry versus crystal packing in N-methyl-N-(2-nitrophenyl) cinnamanilide: An experimental charge density study

ARTICLE in JOURNAL OF MOLECULAR STRUCTURE · JUNE 2000

Impact Factor: 1.6 · DOI: 10.1016/S0022-2860(99)00454-8

CITATIONS

7

READS

9

4 AUTHORS, INCLUDING:



R. Srinivasa Gopalan

Unilever

24 PUBLICATIONS 581 CITATIONS

[SEE PROFILE](#)



Giridhar U Kulkarni

Centre for Nano and Soft Matter Sciences

271 PUBLICATIONS 4,436 CITATIONS

[SEE PROFILE](#)



Easwara Subramanian

University of Madras

110 PUBLICATIONS 1,355 CITATIONS

[SEE PROFILE](#)

Reprinted from

Journal of MOLECULAR STRUCTURE

Journal of Molecular Structure 524 (2000) 169–178

Molecular geometry versus crystal packing in *N*-methyl-*N*-(2-nitrophenyl) cinnamanilide: an experimental charge density study

R.S. Gopalan^a, G.U. Kulkarni^{a,*}, E. Subramanian^b, S. Renganayaki^b

^aChemistry and Physics of Materials Unit, Jawaharlal Nehru Centre for Advanced Scientific Research, Jakkur P.O., Bangalore 560 064, India

^bDepartment of Crystallography and Biophysics, University of Madras, Guindy Campus, Chennai 600 025, India





ELSEVIER

Journal of
MOLECULAR
STRUCTURE

Journal of Molecular Structure 524 (2000) 169–178

www.elsevier.nl/locate/molstruc

Molecular geometry versus crystal packing in *N*-methyl-*N*-(2-nitrophenyl) cinnamanilide: an experimental charge density study

R.S. Gopalan^a, G.U. Kulkarni^{a,*}, E. Subramanian^b, S. Renganayaki^b

^aChemistry and Physics of Materials Unit, Jawaharlal Nehru Centre for Advanced Scientific Research, Jakkur P.O., Bangalore 560 064, India

^bDepartment of Crystallography and Biophysics, University of Madras, Guindy Campus, Chennai 600 025, India

Received 18 August 1999; received in revised form 9 November 1999; accepted 22 November 1999

Abstract

A charge density investigation of *N*-methyl-*N*-(2-nitrophenyl)cinnamanilide has been carried out using X-ray crystallography. The molecular geometry in the solid state is compared with that of a “free” molecule generated using the semi-empirical AM1 calculation. Significant differences are observed in torsion angles, though the bond lengths and angles are quite similar in the two cases. In the solid state, the cinnamide portion of the molecule is quite planar and the nitrobenzene ring is twisted out of this plane. In the “free” molecule, however the two phenyl rings are nearly planar and the bonds joining them are buckled. The molecule in the lattice is bound by C–H···O contacts, the prominent being a pair of centrosymmetrically related bifurcated hydrogen bonds from amidic oxygen. Experimental charge density reveals certain interesting aspects of both intra- and intermolecular bonding. It is observed that there is extensive charge redistribution in the amide group, with the C=O bond carrying relatively high density. Lone-pairs of the amidic oxygen appear to be polarized along the bifurcated hydrogen bonds. The C–H···O bonds from the amidic oxygen are stronger than those from nitro-oxygens. Hydrogen bonding from the amidic oxygen thus dictates molecular structure and packing. © 2000 Elsevier Science B.V. All rights reserved.

Keywords: *N*-methyl-*N*-(2-nitrophenyl)cinnamanilide; Experimental charge density; X-ray crystallography; MOPAC calculation; Bifurcated hydrogen bonds

1. Introduction

Cohesion of molecules in crystalline state has been a topic of great interest for both structural and quantum chemists. It is well known that during crystallization, the lattice imposes restrictions on the conformation and symmetry of the molecules and the molecules often distort so as to maximize the

intermolecular interactions. For instance, the nitrobenzene molecule, which is known to be planar in the free state [1] is twisted by ~2° in the solid state [2] across the nitrobenzene link. On the contrary, biphenyl is non-planar in both gaseous [3] and liquid [4] states, while it is planar in the crystal [5,6] at room temperature, exhibiting D_{2h} symmetry compared to D_2 in the former cases. Another example of the effect of lattice on the molecular structure is illustrated in a recent study on dimorphism in tetraphenylpyrazine [7]. This molecule possesses an inversion center in one form and a two-fold axis in the other. There are

* Corresponding author. Tel.: +91-80-846-2750; fax: +91-80-846-2766.

E-mail address: kulkarni@jncasr.ac.in (G.U. Kulkarni).

Table 1
Crystal data and experimental details

Crystal	Cinnamanilide
Chemical formula	C ₁₆ H ₁₄ N ₂ O ₃
Formula weight (g)	282.29
Cell system	Monoclinic
Space group	P2(1)/n
a (Å)	10.3397(1)
b (Å)	10.0008(1)
c (Å)	13.8310(1)
β (°)	107.019(1)
V (cm ³)	1367.6(4)
Z	4
ρ (g cm ⁻³)	1.371
Radiation type	MoKα
Wavelength (Å)	0.71073
No. of reflections for cell parameters	60
μ (mm ⁻¹)	0.1
Crystal form	Cuboidal
Crystal size (mm)	0.45 × 0.3 × 0.5
Crystal color	Colorless
Data collection temperature	130 K
Diffractometer	Siemens CCD
Crystal-detector distance (cm)	5.0
No. of measured reflections	22 993
No. of independent reflections	11 258
No. of observed reflections	7936
R _{merge}	0.0369
R _{int}	0.0298
θ _{max} (°)	49.43
Range of h, k, l	-19 ≤ h ≤ 21 -20 ≤ k ≤ 19 -29 ≤ l ≤ 29
Refinement	
R ₁	0.0464
wR ₂	0.0668
S	1.0876
No. of variables	393
N _{ref} /N _v	36.1

several such examples. It is of considerable importance, therefore, to understand the symmetries prevailing in a molecular solid in terms of the distortion of the molecules and the nature of intermolecular interactions. In this context, we have investigated N-methyl-N-(2-nitrophenyl)cinnamanilide, which exhibits a highly favored bifurcated hydrogen bonded ring structure in the lattice and is also considerably distorted [8]. In continuation of our studies of molecular solids using experimental charge density [9], it was of our interest to examine molecular distortion

and bonding in N-methyl-N-(2-nitrophenyl)cinnamanilide. For this purpose, we have carried out a high-resolution X-ray diffraction measurement at 130 K and analyzed the charge densities in the intramolecular as well intermolecular regions. We have also compared the structure of the molecule in the lattice with that in the free state obtained by geometry optimization. Our study has shown that hydrogen bond interactions from the amide oxygen supersede those from nitro-oxygens leading to the distortion of the molecule relative to the free state.

2. Experimental

N-methyl-N-(2-nitrophenyl)cinnamanilide was prepared following the procedure described in Ref. [8]. Crystals of this compound were obtained from a mixture of hexane and dichloromethane. A high quality crystal was chosen after examination under an optical microscope. X-ray diffraction intensities were measured by ω scans using a Siemens three-circle diffractometer attached with a CCD area detector and a graphite monochromator for the MoKα radiation (50 kV, 40 mA). The crystals were cooled to 130 K on the diffractometer using a stream of cold nitrogen gas from a vertical nozzle and this temperature was maintained throughout the data collection.

The unit cell parameters and the orientation matrix of the crystal were initially determined using ~60 reflections from 25 frames collected over a small ω scan of 7.5° sliced at 0.3° interval. A hemisphere of reciprocal space was then collected in two shells using the SMART software [10] with 2θ settings of the detector at 28 and 70. Data reduction was performed using the SAINT program [10] and the orientation matrix along with the detector and the cell parameters were refined for every 40 frames on all the measured reflections. The various experimental details are listed in Table 1. The crystal structure was first determined with the low-resolution data up to $\sin \theta/\lambda = 0.56 \text{ Å}^{-1}$. The phase problem was solved by direct methods and the non-hydrogen atoms were refined anisotropically, by means of the full matrix least squares procedures using SHELXTL program [11]. All the hydrogens were located using the difference Fourier method and the temperature factors of the hydrogens were refined

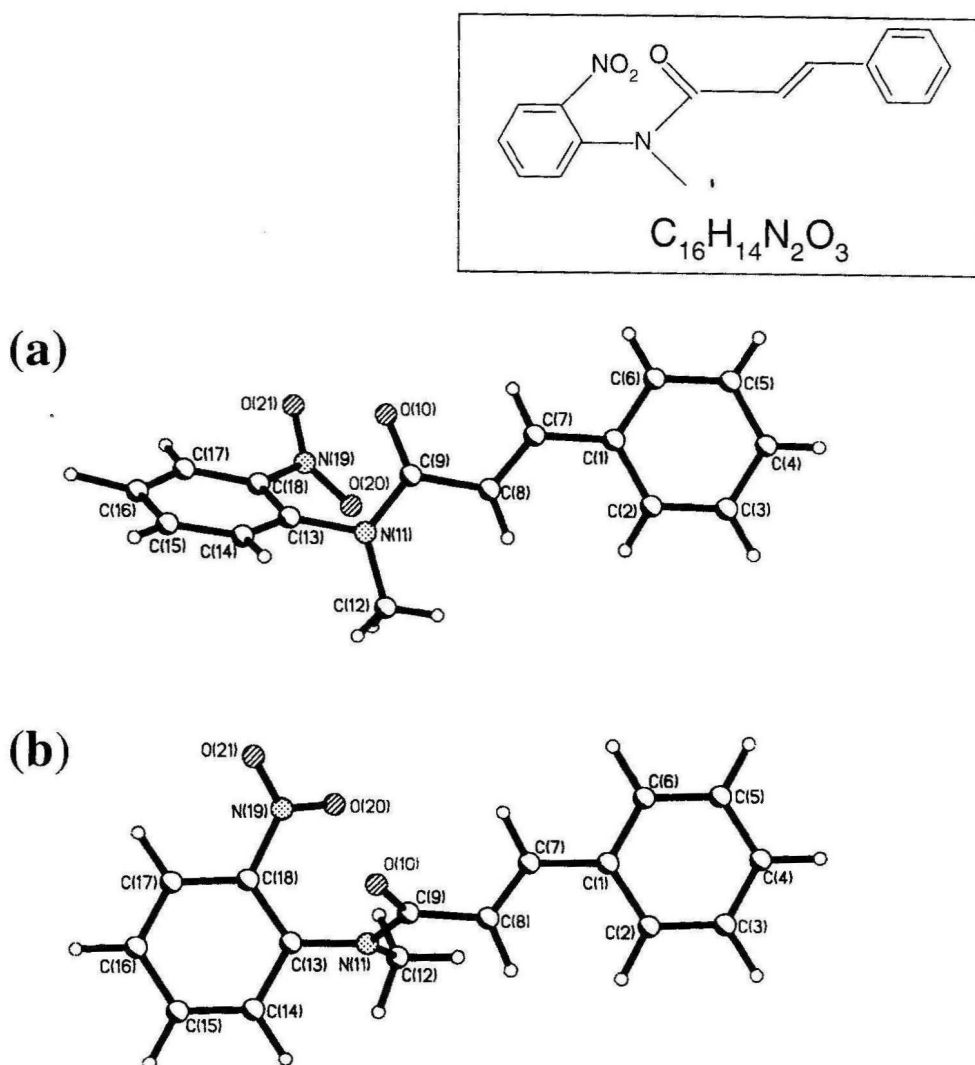


Fig. 1. Molecular structure of *N*-methyl-*N*-(2-nitrophenyl)cinnamanilide from (a) X-ray crystallography; and (b) AM1 calculation. Formula diagram is shown in the inset on the top.

isotropically. The structure so obtained was found to be in good agreement with the structure reported previously [8].

Charge density analysis was carried out based on multipole expansion of the electron density centered at the nucleus of the atom [12]. Accordingly, the aspherical atomic density can be described in terms of spherical harmonics,

$$\rho_{\text{atom}}(r) = \rho_{\text{core}}(r) + \rho_{\text{valence}}(r) + \rho_{\text{def}}(r)$$

Thus for each atom,

$$\begin{aligned} \rho_{\text{atom}}(r) &= \rho_{\text{core}}(r) + P_v \kappa^3 \rho_{\text{valence}}(\kappa r) \\ &\quad + \sum_{l=0} \kappa'^3 R_l(\kappa' \zeta r) \sum_{m=0} \sum_{p=\pm l} P_{lmp} Y_{lmp}(\theta, \varphi) \end{aligned}$$

with the origin at the atomic nucleus. The population coefficients, P_{lmp} are to be refined along with the κ and κ' parameters which control the radial dependence of the valence shell density. The analysis was carried out in several steps.

Table 2

Bond lengths, bond angles and torsion angles involving non-hydrogen atoms from X-ray crystallography and AM1 calculation

<i>Bond length (Å)</i>	X-ray	AM1 calculation
C(1)–C(2)	1.414(2)	1.4029
C(1)–C(6)	1.407(1)	1.4044
C(1)–C(7)	1.482(1)	1.4536
C(2)–C(3)	1.407(1)	1.394
C(3)–C(4)	1.402(2)	1.3945
C(4)–C(5)	1.397(2)	1.3932
C(5)–C(6)	1.412(2)	1.3969
C(7)–C(8)	1.354(1)	1.3413
C(8)–C(9)	1.497(1)	1.4837
C(9)–O(10)	1.241(2)	1.2455
C(9)–N(11)	1.373(1)	1.404
N(11)–C(12)	1.466(2)	1.4398
N(11)–C(13)	1.445(1)	1.4218
C(13)–C(14)	1.406(1)	1.4125
C(13)–C(18)	1.394(1)	1.4182
C(14)–C(15)	1.412(2)	1.3894
C(15)–C(16)	1.390(2)	1.3961
C(16)–C(17)	1.407(2)	1.389
C(17)–C(18)	1.408(2)	1.4069
C(18)–N(19)	1.479(1)	1.4899
N(19)–O(20)	1.243(2)	1.2022
N(19)–O(21)	1.225(2)	1.2012
<i>Bond angle (°)</i>		
C(6)–C(1)–C(7)	119.14(9)	118.85
C(2)–C(1)–C(7)	122.79(8)	122.04
C(2)–C(1)–C(6)	118.03(9)	119.1
C(1)–C(2)–C(3)	120.79(9)	120.39
C(2)–C(3)–C(4)	120.5(1)	120.23
C(3)–C(4)–C(5)	119.3(1)	119.82
C(4)–C(5)–C(6)	120.4(1)	120.29
C(1)–C(6)–C(5)	121.0(1)	120.17
C(1)–C(7)–C(8)	125.8(1)	124.83
C(7)–C(8)–C(9)	119.8(1)	120.35
C(8)–C(9)–N(11)	118.8(1)	118.16
C(8)–C(9)–O(10)	121.8(1)	121.99
O(10)–C(9)–N(11)	119.4(1)	119.79
C(9)–N(11)–C(13)	117.7(1)	119.24
C(9)–N(11)–C(12)	127.0(1)	122.44
C(12)–N(11)–C(13)	115.3(1)	115.77
N(11)–C(13)–C(18)	122.5(1)	123.3
N(11)–C(13)–C(14)	120.3(1)	118.94
C(14)–C(13)–C(18)	117.2(1)	117.75
C(13)–C(14)–C(15)	121.7(1)	121.02
C(14)–C(15)–C(16)	120.0(1)	120.48
C(15)–C(16)–C(17)	119.3(1)	120.05
C(16)–C(17)–C(18)	119.7(1)	119.91
C(13)–C(18)–C(17)	122.0(1)	120.77
C(17)–C(18)–N(19)	118.3(1)	117.54
C(13)–C(18)–N(19)	119.7(1)	121.69
C(18)–N(19)–O(21)	117.1(1)	118.41
C(18)–N(19)–O(20)	118.8(1)	119.78

Table 2 (continued)

<i>Bond angle (°)</i>	X-ray	AM1 calculation
O(20)–N(19)–O(21)	124.1(1)	121.75
<i>Torsion angle (°)</i>		
C(6)–C(1)–C(7)–C(8)	171.9(1)	160.92
C(2)–C(1)–C(7)–C(8)	−6.2(2)	−19.69
C(7)–C(1)–C(6)–C(5)	−176.9(1)	−179.85
C(2)–C(1)–C(6)–C(5)	1.3(2)	0.74
C(6)–C(1)–C(2)–C(3)	−0.2(2)	−0.34
C(7)–C(1)–C(2)–C(3)	177.9(1)	−179.72
C(1)–C(2)–C(3)–C(4)	−0.9(2)	−0.14
C(2)–C(3)–C(4)–C(5)	0.9(2)	0.22
C(3)–C(4)–C(5)–C(6)	0.2(2)	0.19
C(4)–C(5)–C(6)–C(1)	−1.3(2)	−0.67
C(1)–C(7)–C(8)–C(9)	−176.4(1)	178.64
C(7)–C(8)–C(9)–O(10)	2.9(2)	−42.31
C(7)–C(8)–C(9)–N(11)	−177.4(1)	140.58
C(8)–C(9)–N(11)–C(12)	−3.8(2)	−22.39
C(8)–C(9)–N(11)–C(13)	179.2(1)	176.46
O(10)–C(9)–N(11)–C(13)	175.9(1)	160.43
O(10)–C(9)–N(11)–O(10)	−1.0(1)	−0.72
N(11)–C(13)–C(12)–N(11)	−111.2(1)	−111.42
C(9)–N(11)–C(12)–C(13)	68.4(1)	67.74
C(13)–C(12)–N(11)–C(13)	71.5(1)	86.21
C(12)–N(11)–C(13)–C(18)	−109.0(1)	−94.63
C(13)–C(12)–N(11)–C(18)	121.02	123.3
N(11)–C(13)–C(18)–C(13)	0.6(1)	2.18
C(18)–C(17)–N(11)–C(13)	−179.5(1)	−177.34
C(18)–C(17)–N(11)–C(18)	−178.1(1)	178.5
C(14)–C(15)–C(16)–C(17)	121.69	C(14)–C(15)
C(14)–C(13)–C(18)–N(19)	−179.8(1)	−178.64
C(18)–N(19)–O(20)–C(18)	C(18)–N(19)	

Table 2 (continued)

Torsion angle (°)	X-ray	AM1 calculation
C(14)–C(13)–	0.1(2)	1.83
C(18)–C(17)		
C(18)–C(13)–	2.3(2)	−0.71
C(14)–C(15)		
C(13)–C(14)–	−2.1(2)	−0.45
C(15)–C(16)		
C(14)–C(15)–	−0.5(2)	0.51
C(16)–C(17)		
C(15)–C(16)–	2.8(2)	0.62
C(17)–C(18)		
C(16)–C(17)–	−2.7(2)	−1.81
C(18)–C(13)		
C(16)–C(17)–	177.3(1)	178.65
C(18)–N(19)		
C(17)–C(18)–	−136.5(1)	−145.31
N(19)–O(20)		
C(13)–C(18)–	43.5(2)	35.15
N(19)–O(20)		
C(17)–C(18)–	42.2(2)	31.89
N(19)–O(21)		
C(13)–C(18)–	−137.8(1)	−147.65
N(19)–O(21)		

A high order refinement of the data was first performed using reflections with $\sin \theta/\lambda \geq 0.6 \text{ \AA}^{-1}$ and $F_0 \geq 4\sigma$. The Hydrogen atom positions were found using the difference Fourier method and were adjusted to average neutron values as is usually done during the multipole refinement (C_{sp^3} –H, 1.06 Å; C_{sp^2} –H, 1.075 Å). The non-hydrogen atoms were treated anisotropically. All the hydrogens were held constant throughout the refinement along with their isotropic temperature factors. Rigid body analysis was carried out using THMA routine of PLATON program [13]. All the bonds closely satisfied the Hirshfeld criterion [14] except C(2)–C(3) which deviated marginally ($\Delta_{ij} \sim 0.0014 \text{ \AA}$). Multipolar refinement for the charge density analysis was carried out using the XDLSM routine of the XD package [15] and the details are given in Table 1. The atomic coordinates and the thermal parameters obtained from the high-order refinement were used as input to XD refinement. Carbon, nitrogen and oxygen atoms were refined up to octapole moments while hydrogens were restricted to dipole. Kappa refinement was carried out on the valence shells of the non-hydrogen atoms. The static deformation density, $\Delta\rho$, was obtained as the difference between the total density

and the spherical density without the thermal smearing. The deformation density maps were plotted using the XDGRAPH routine. The residual maps in different planes of the molecule were featureless, the magnitude of the highest residual peak being $\sim 0.2e \text{ \AA}^{-3}$. The XDPROP routine was used to calculate the total electron density, $\rho(r)$, the Laplacian, $\nabla^2\rho$, and the ellipticity, ϵ , at the bond critical points (CPs). The value of ρ_{CP} is a measure of bond strength while the Laplacian signifies the extent of depletion or concentration of bonding density. Ellipticity measures the extent of conjugation. All the intramolecular CPs were of (3, −1) type in $\rho(r)$ with negative Laplacians, characteristic of covalently bonded molecular systems [16]. The lone-pair electrons were located as (3, +3) CPs in $\nabla^2\rho$. Intermolecular hydrogen contacts as determined by the PARST [17] program were analyzed.

3. Results and discussion

The molecule, *N*-methyl-*N*-(2-nitrophenyl) cinnamanilide, crystallizes in a monoclinic cell ($a = 10.3397(1) \text{ \AA}$, $b = 10.0008(1) \text{ \AA}$, $c = 13.8310(1) \text{ \AA}$, $\beta = 107.019(1)^\circ$). There are four molecules in the unit cell (Table 1). In Fig. 1a we show the molecular structure of the cinnamanilide, which is also the asymmetric unit. The most striking feature is that the molecule is twisted at the amide–phenyl (N(11)–C(13)) link with the cinnamide portion being nearly planar (torsion angle C(2)–C(1)–C(7)–C(8), $−6.24^\circ$). The nitrobenzene ring is highly non-planar, the nitro group being rotated with respect to the phenyl ring by 43.5° . The nitrobenzene group as a whole is twisted away from the mean cinnamide plane making an angle of 63.3° . The molecular structure in the lattice as discussed above, was compared with that of a “free” molecule, shown in Fig. 1b. The latter was obtained using a semi-empirical calculation (AM1, PRECISE) after optimizing bond lengths, angles and torsion angles using MOPAC [1]. The experimental coordinates served as the initial input. SCF was achieved and the heat of formation and the dipole moments of the molecule so obtained are $49.73 \text{ kcal mol}^{-1}$ and 5.215 Debye , respectively. An important finding from the calculation is that the benzene rings are parallel within 8° while the intervening bonds are buckled with torsion angles from

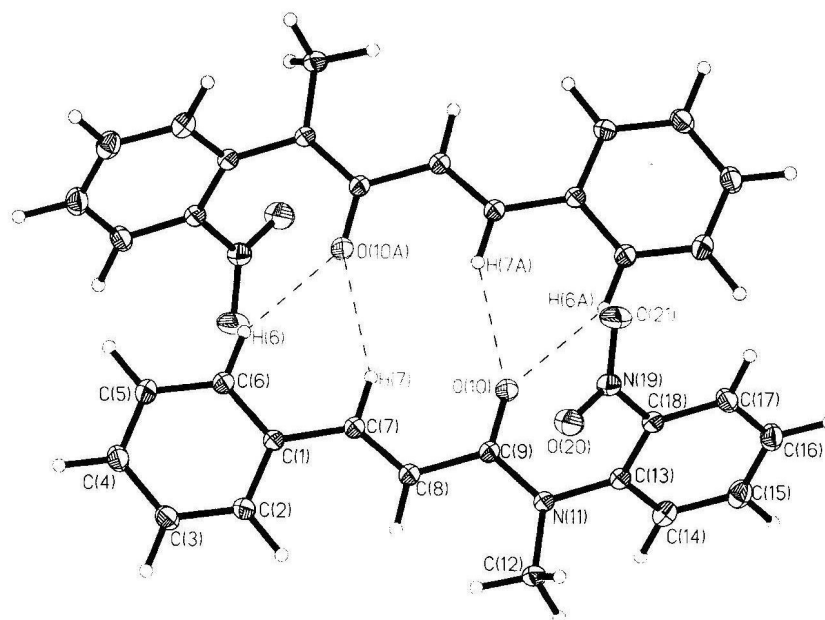


Fig. 2. Bifurcated hydrogen bonds in the intermolecular region of centrosymmetrically related molecules. All non-hydrogen atoms are shown at 50% probability ellipsoids.

$C(2)-C(1)-C(7)-C(8)$ through $C(8)-C(9)-N(11)-C(13)$ being -19.69 , 178.64 , 140.58 and 176.46° , respectively as compared to -6.24 , -176.36 , -177.31 and 179.24° in solid state (Table 2). The $O(10)-C(9)-N(11)-C(12)$ torsion angle is 160.83° as compared to 175.95° found in solid state. However,

the bond lengths and angles are quite similar in the two cases (see Table 2). Thus, our calculation provides a reference state of the molecule using which constraints imposed by packing in a lattice could be examined.

In Fig. 2 we show two centrosymmetrically related

Table 3
Intermolecular hydrogen bond contacts

D-H···A	Bond type	H···A (Å)	D···A (Å)	$\angle D-H\cdots A$ ($^\circ$)
$C(6)-H(6)\cdots O(10)^a$	$R_1^2(6)$	2.369(1)	3.362(1)	152.7(1)
$C(7)-H(7)\cdots O(10)^a$	$R_1^2(6)$	2.440(1)	3.410(1)	149.3(1)
$C(17)-H(17)\cdots O(10)^b$	$D(2)$	2.331(2)	3.330(1)	153.7(1)
$C(16)-H(16)\cdots O(10)^c$	$D(2)$	2.896(1)	3.741(1)	135.5(1)
$C(4)-H(4)\cdots O(20)^d$	$D(2)$	2.695(1)	3.606(1)	142.2(1)
$C(2)-H(2)\cdots O(20)^e$	$R_1^2(7)$	2.598(1)	3.622(1)	166.3(1)
$C(8)-H(8)\cdots O(20)^e$	$R_1^2(7)$	2.758(1)	3.785(1)	159.4(1)
$C(12)-H(12C)\cdots O(20)^e$	$R_1^2(7)$	2.723(1)	3.692(1)	151.9(1)
$C(15)-H(15)\cdots O(21)^c$	$R_1^2(5)$	2.802(1)	3.529(1)	124.9(1)
$C(16)-H(16)\cdots O(21)^c$	$R_1^2(5)$	2.916(1)	3.579(1)	120.1(1)

^a $-x, 1-y, -z$.

^b $1/2-x, 1/2+y, 1/2-z$.

^c $1/2+x, 3/2-y, 1/2+z$.

^d $-1-x, 1-y, -z$.

^e $-1/2-x, -1/2+y, 1/2-z$.

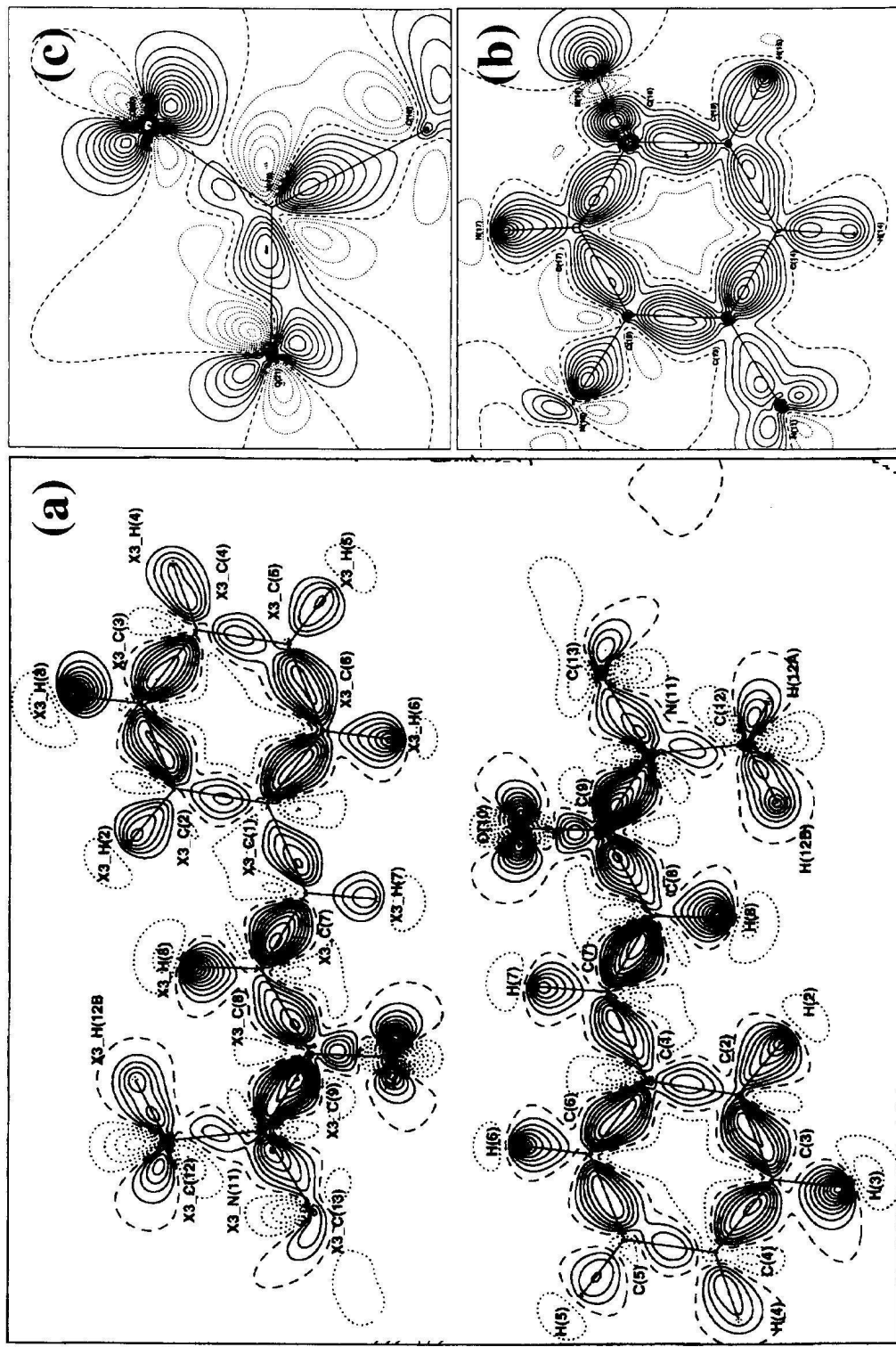


Fig. 3. Deformation density map of *N*-methyl-*N'*-(2-nitrophenyl)cinnamanimide close to the mean plane of (a) bifurcated hydrogen bond; (b) nitrobenzene ring; and (c) nitro group. Contour intervals at $0.1e\text{\AA}^{-3}$.

Table 4
Analysis of the bond critical points

Bond	ρ ($e \text{ \AA}^{-3}$)	$\nabla^2 \rho$ ($e \text{ \AA}^{-5}$)	ϵ
C(1)–C(2)	1.83(2)	-12.40(5)	0.12
C(2)–C(3)	2.08(2)	-15.01(5)	0.28
C(3)–C(4)	2.10(2)	-16.07(6)	0.19
C(4)–C(5)	1.91(3)	-11.64(6)	0.22
C(5)–C(6)	2.15(2)	-18.43(5)	0.11
C(1)–C(6)	2.11(2)	-17.88(5)	0.24
C(2)–H(2)	1.82(5)	-18.0(1)	0.09
C(3)–H(3)	1.59(4)	-10.7(1)	0.07
C(4)–H(4)	1.77(5)	-15.8(2)	0.03
C(5)–H(5)	1.76(6)	-19.6(3)	0.06
C(6)–H(6)	1.74(5)	-16.3(1)	0.09
C(1)–C(7)	1.81(2)	-12.26(4)	0.19
C(7)–C(8)	2.35(2)	-21.24(6)	0.23
C(8)–C(9)	1.72(2)	-9.71(4)	0.3
O(10)–C(9)	2.56(6)	-13.2(1)	0.05
N(11)–C(9)	2.45(2)	-17.42(6)	0.21
N(11)–C(12)	1.49(3)	-2.03(7)	0.17
N(11)–C(13)	1.92(3)	-10.56(7)	0.08
C(7)–H(7)	1.67(4)	-13.1(1)	0.04
C(8)–H(8)	1.61(5)	-11.8(1)	0.02
C(12)–H(12A)	1.71(5)	-11.3(1)	0.31
C(12)–H(12B)	1.69(6)	-12.3(2)	0.19
C(12)–H(12C)	1.61(6)	-13.1(3)	0.14
C(13)–C(14)	2.11(3)	-18.03(8)	0.13
C(14)–C(15)	2.07(3)	-15.82(6)	0.15
C(15)–C(16)	2.21(3)	-17.92(6)	0.12
C(16)–C(17)	2.02(3)	-15.37(9)	0.11
C(17)–C(18)	2.20(2)	-19.82(6)	0.14
C(13)–C(18)	2.17(2)	-19.06(6)	0.15
C(14)–H(14)	1.79(6)	-18.2(2)	0.05
C(15)–H(15)	1.77(6)	-17.1(3)	0.05
C(16)–H(16)	1.31(6)	3.7(3)	0.64
C(17)–H(17)	1.85(5)	-18.8(1)	0.06
N(19)–C(18)	1.71(3)	-10.13(8)	0.17
O(20)–N(19)	2.85(9)	5.2(1)	0.14
O(21)–N(19)	3.3(1)	-6.7(2)	0.2

molecules in the unit cell involved in hydrogen bonding. We see that each molecule forms bifurcated C–H···O hydrogen bonds [18] with the amidic oxygen of the centrosymmetric partner. The contacts from H(6) and H(7) are at 2.369 and 2.440 Å with C–H···O angle of 149.3 and 152.7°, respectively (Table 3). The angle of bifurcation is ~60.4°. These hydrogen bonds are of R₁²(6) type [19–21] and the two pairs are related by a center of inversion. As expected of a bifurcated hydrogen bond, the atoms H(6), H(7), O(10A) and C(9A) are coplanar [22] within 0.0161 Å. In addition to ring hydrogen

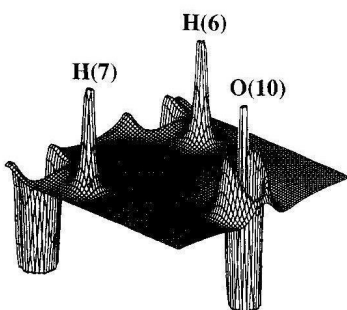


Fig. 4. Relief map of the negative Laplacian in the plane of the bifurcated hydrogen bond. Range, -250 to 250 $e \text{ \AA}^{-5}$.

bonds, the amidic oxygen forms hydrogen contact of D(2) type with phenyl hydrogens, H(16) and H(17). The latter contact appears to be more favorable (2.331 Å, 153.7°). Besides those from the amidic oxygen, there exist C–H···O contacts from the nitro-oxygens as well (see Table 3). It may be noted that the intermolecular bonding in this crystal is only through C–H···O contacts.

We now discuss the charge density analysis of both the intra- and intermolecular regions. In Fig. 3, we show the deformation map of the molecule in three parts (a, b and c) since it is highly non-planar. Concentric contours typify the various bonding regions in the molecules between the atom-cores. The charge density distribution is as expected in the various regions of the molecule (Table 4). However, a few points are noteworthy. The topography of the deformation density in the C(7)=C(8) region is distinctly different from those of the neighboring single bonds (Fig. 3a). Accordingly, the charge density at the CP is typical of an isolated double bond¹ ($\rho = 2.349 e \text{ \AA}^{-3}$, $\nabla^2 \rho = -21.24 e \text{ \AA}^{-5}$, $\epsilon = 0.23$). The other region of interest is that of the amide group (Fig. 3a). The methyl (C(12)–N(11)) and the amidic link (C(9)–N(11)) exhibit widely differing densities (1.49 and 2.45 $e \text{ \AA}^{-3}$, respectively), though both are C–N bonds. Theoretical estimation [25] of bonding density of a C–N bond is 1.86 $e \text{ \AA}^{-3}$. Thus, it appears as though the density has migrated from the methyl link to the amidic region. The density

¹ Although the cinnamoyl group may be potentially reactive with its centrosymmetric partner this may not be the case here. We find that the distance ~5.266 Å is well above the Schmidt's criterion [23] and that the double bond is localized [24].

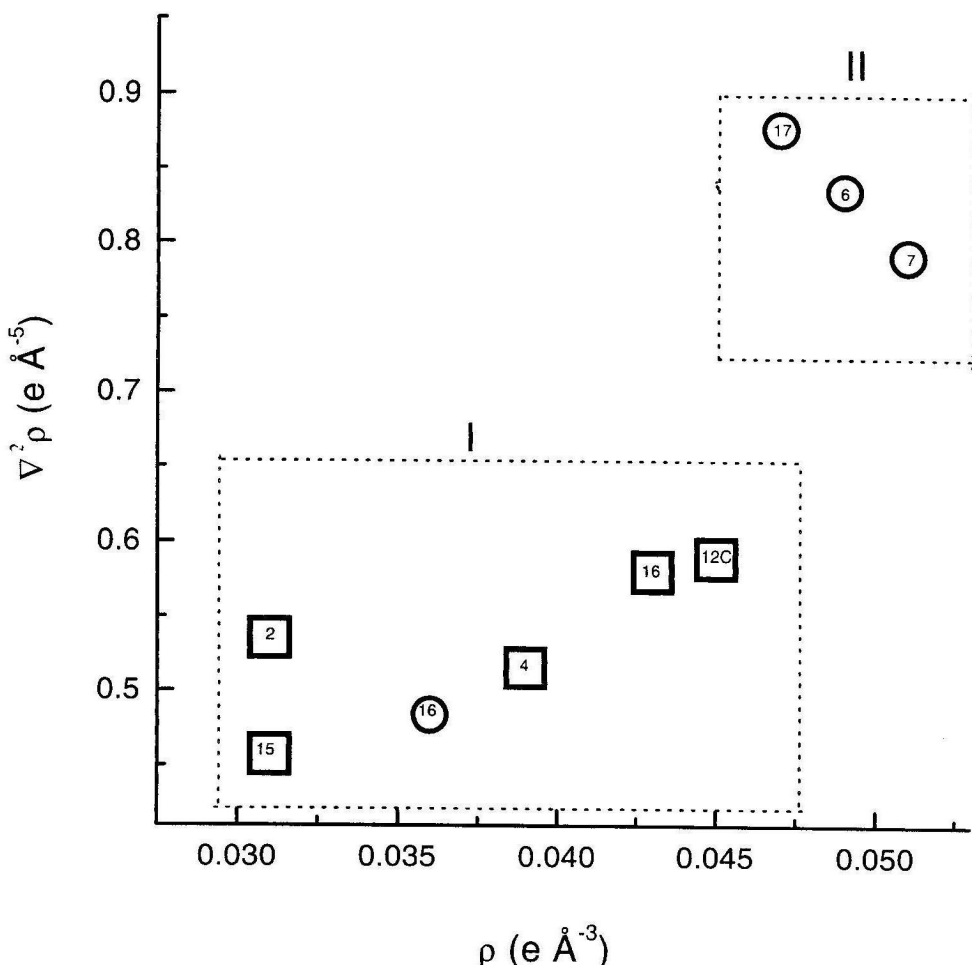


Fig. 5. Variation of $\nabla^2 \rho_{CP}$ with ρ_{CP} for various hydrogen bonds, $O_{\text{amido}} \cdots H$, circles; $O_{\text{nitro}} \cdots H$, squares. The numbers inside the symbols refer to the hydrogens involved in bonding. Regions I and II emphasize different trends in the plot.

in the $C(9)=O(10)$ bond is also somewhat high, $2.56e \text{ \AA}^{-3}$. In Fig. 3c, we find that there is very little deformation density in the N–O bonds, which is due to ionic interactions. This is reflected in the low values of the Laplacians (see Table 4). We also find that the nitro-oxygens carry higher charges ($O(20)$, $-0.30e$; $O(21)$, $-0.1e$) compared to the amidic oxygen ($-0.06e$).

The lone-pair electrons around the amidic oxygen, $O(10)$ (Fig. 3a) and the nitro-oxygens (Fig. 3c) are clearly visible as two sets of concentric contours around each nucleus. In Laplacian, they were found to occur as (3, +3) CPs exhibiting high Laplacians

$\sim -220e \text{ \AA}^{-5}$. The distance of the CP from the nucleus is ~ 0.31 and 0.38 \AA in the case of $O(10)$ and nitro-oxygens, respectively. The relief map of the Laplacian shown in Fig. 4, reveals that the lone-pair density around $O(10)$ is slightly polarized towards $H(6)$ and $H(7)$, involved in bifurcated hydrogen bonding. This is also evident from the deformation density map in Fig. 3a where the contours of the lone-pair are seen oriented towards the hydrogens. These hydrogen bonds carry a small density of $\sim 0.05e \text{ \AA}^{-3}$ and small positive Laplacians, $\sim 0.8e \text{ \AA}^{-5}$, typical of closed shell interactions [26]. The hydrogen bonding between the phenyl hydrogen

H(17) and the amidic oxygen O(10) forms the next strongest hydrogen bond with a density of $0.047e\text{ \AA}^{-3}$ and a Laplacian of $0.877e\text{ \AA}^{-5}$. We find that the oxygens of the nitro group exhibit much weaker hydrogen bonds ($\rho_{\text{mean}} = 0.034e\text{ \AA}^{-3}$ and $\nabla^2\rho = 0.526e\text{ \AA}^{-5}$).

The trends associated with the various hydrogen bonds are better understood by plotting $\nabla^2\rho$ versus ρ [27,28] (Fig. 5). We could clearly mark two regions of interactions as shown—one region where the hydrogen bonds exhibit low values for both the density and the Laplacian and the other, where both quantities are disproportionately higher. What is interesting is that all the bonds involving the nitro-oxygens belong to the first region and those from the amidic oxygen fill the second region. Clearly, the amidic oxygen forms stronger hydrogen bonds compared to the more ionic nitro-oxygens. This appears to govern the molecular geometry and packing in the solid state.

4. Conclusions

1. *N*-methyl-*N*-(2-nitrophenyl)cinnamanilide crystallizes in $P2(1)/n$ and exhibits centrosymmetrically related $R_j^6(6)$ hydrogen bond ring structure in the intermolecular region.
2. The amidic oxygen appears to be the active center for hydrogen bonding with both ρ and $\nabla^2\rho$ being higher as compared to those involving nitro-oxygens.
3. It is as though to favor bifurcated hydrogen bonding from the amidic oxygen, the molecule is highly twisted at the amide–nitrobenzene link. Semi-empirical calculations show that in the “free” molecule, the two phenyl rings are coplanar within 8° while the intervening groups are buckled out of plane.

Acknowledgements

The authors thank Professor C.N.R. Rao, F.R.S. for useful discussions. R.S.G and G.U.K are grateful to him for his encouragement.

References

- [1] J.J.P. Stewart, *J. Comput.-Aided Mol. Des.* 4 (1990) 1.
- [2] R. Bosse, D. Balser, M. Nussbaumer, T.M. Krygowski, *Struct. Chem.* 3 (1992) 362.
- [3] O. Bastiansen, *Acta Chem. Scand.* 3 (1949) 408.
- [4] V.J. Eaton, D.J. Steele, *J. Chem. Soc., Faraday Trans.* 69 (1973) 1601.
- [5] A. Chakrabarti, S. Yashonath, C.N.R. Rao, *Mol. Phys.* 84 (1995) 49.
- [6] J. Trotter, *Acta Cryst.* 14 (1961) 1135.
- [7] R. Bartnik, R. Faure, K. Gebicki, *Acta Cryst. C* 55 (1999) 1034.
- [8] E. Subramanian, S. Renganayaki, S.S.S. Raj, H.-K. Fun, *Acta Cryst. C* 55 (1999) 764.
- [9] G.U. Kulkarni, P. Kumaradhas, C.N.R. Rao, *Chem. Mater.* 10 (1998) 3498.
- [10] Siemens Analytical X-ray Instruments Inc. 1995, Madison, Wisconsin, USA.
- [11] SHEXLTL (SGI version) Siemens Analytical X-ray Instruments Inc. 1995, Madison, WI, USA.
- [12] N.K. Hansen, P. Coppens, *Acta Cryst. A* 34 (1978) 909.
- [13] A.L. Spek, *Acta Cryst. A* 46 (1990) C34.
- [14] H.L. Hirshfeld, *Acta Cryst. A* 32 (1976) 239.
- [15] T. Koritsansky, S.T. Howard, T. Richter, P.R. Mallinson, Z. Su, N.K. Hansen, XD, A computer program package for Multipole Refinement and Analysis of charge densities from diffraction data, Cardiff, Glasgow, Buffalo, Nancy, Berlin.
- [16] R.F.W. Bader, H.J. Essen, *J. Chem. Phys.* 80 (1984) 1943.
- [17] M. Naradelli, *Comput. Chem.* 7 (1983) 95.
- [18] I. Rozas, I. Alkorta, J. Elguero, *J. Phys. Chem. A* 102 (1998) 9925.
- [19] M.C. Etter, *Acc. Chem. Res.* 23 (1990) 120.
- [20] M.C. Etter, J.C. MacDonald, *Acta Cryst. B* 46 (1990) 256.
- [21] J. Bernstein, R.E. Davis, L. Shimoni, N-L. Chang, *Angew. Chem. Int. Ed. Engl.* 34 (1995) 1555.
- [22] R. Parthasarathy, *Acta Cryst. B* 25 (1969) 509.
- [23] M.D. Cohen, G.M.J. Schmidt, F.I. Sonntag, *J. Chem. Soc.* (1964) 2000.
- [24] R.S. Gopalan, G.U. Kulkarni, C.N.R. Rao, submitted for publication.
- [25] D. Cremer, E. Kraka, *Croat. Chem. Acta* 57 (1984) 1259.
- [26] R.F.W. Bader, *Atoms in Molecules—a Quantum Theory*, Clarendon Press, Oxford, 1990.
- [27] P.R. Mallinson, K. Wozniak, T. Garry, K.L. McCormack, *J. Am. Chem. Soc.* 119 (1997) 11 502.
- [28] R.S. Gopalan, P. Kumaradhas, G.U. Kulkarni, C.N.R. Rao, *J. Mol. Struct.* (2000) in press.